# γ-Parvin Is Dispensable for Hematopoiesis, Leukocyte Trafficking, and T-Cell-Dependent Antibody Response†

Haiyan Chu,[1] Ingo Thievessen,[1] Michael Sixt,[1] Tim Lämmermann,[1] Ari Waisman,[2]‡
Attila Braun,[1] Angelika A. Noegel,[3] and Reinhard Fässler[1]*

*Department of Molecular Medicine, Max Planck Institute for Biochemistry, Am Klopferspitz 18, 82152 Martinsried, Germany[1];
Laboratory of Molecular Immunology, Institute for Genetics, University of Cologne, Zülpicher Str. 47,
50674 Cologne, Germany[2]; and Center for Biochemistry, Medical Faculty, University of Cologne,
Joseph-Stelzmann-Str. 52, 50931 Cologne, Germany[3]*

**Integrins regulate cell behavior through the assembly of multiprotein complexes at the site of cell adhesion. Parvins are components of such a multiprotein complex. They consist of three members (α-, β-, and γ-parvin), form a functional complex with integrin-linked kinase (ILK) and PINCH, and link integrins to the actin cytoskeleton. Whereas α- and β-parvins are widely expressed, γ-parvin has been reported to be expressed in hematopoietic organs. In the present study, we report the expression pattern of the parvins in hematopoietic cells and the phenotypic analysis of γ-parvin-deficient mice. Whereas α-parvin is not expressed in hematopoietic cells, β-parvin is only found in myeloid cells and γ-parvin is present in both cells of the myeloid and lymphoid lineages, where it binds ILK. Surprisingly, loss of γ-parvin expression had no effect on blood cell differentiation, proliferation, and survival and no consequence for the T-cell-dependent antibody response and lymphocyte and dendritic cell migration. These data indicate that despite the high expression of γ-parvin in hematopoietic cells it must play a more subtle role for blood cell homeostasis.**

Cell extracellular matrix (ECM) adhesions are crucial for various biological processes, including cell migration, proliferation, and cell survival (12, 15, 17). Integrins connect the ECM to the actin cytoskeleton at cellular attachment plaques that contain focal adhesion (FA)-associated proteins (8). A family of proteins consisting of actopaxin/CH-ILKBP/α-parvin, affixin/β-parvin, and γ-parvin, collectively called the parvins, has been recently identified in humans and mice (22, 23, 31, 34). In lower organisms such as *Caenorhabditis elegans* and *Drosophila melanogaster*, there is only a single parvin protein (19, 23). Parvins are composed of an N-terminal polypeptide stretch, followed by a single actin-binding domain, which consists of two in tandem arranged calponin homology domains. α- and β-parvin share a high homology (23), and both bind to integrin-linked kinase (ILK), paxillin, and F-actin at FAs (1, 9, 22, 23, 31, 34). In addition, β-parvin also binds α-PIX, a guanine exchange factor for Rac and Cdc42 (21, 25), and α-actinin (35). Both α- and β-parvin associate with ILK and PINCH to form the ILK-PINCH-parvin complexes (37, 39, 40). Disruption of the complex in mammalian cells alters cell shape and impairs cell motility and survival (7, 36, 38, 39). In *C. elegans* disruption of the complex causes muscle detachment and a PAT (paralyzed at the four-cell stage) phenotype (19).

γ-Parvin consists of 331 amino acids and shares the same protein structure as α- and β-parvin. The mouse γ-parvin only shows 40% identity and 60% similarity to the α- or β-parvin at the amino acid level. No γ-parvin binding partners have been identified thus far. In contrast to the wide expression pattern of α- and β-parvin, γ-parvin mRNA is predominantly found in hematopoietic and lymphoid tissues (16, 22, 23, 34). These features of the γ-parvin raise the question of whether γ-parvin mediates integrin signaling via association with ILK and thereby regulates events, including cell differentiation, migration, and positioning in the hematopoietic system. In the present study, we described the expression pattern of the parvin protein family in hematopoietic organs and hematopoietic cells. To directly test the function of γ-parvin in vivo, we generated γ-parvin-deficient mice. Our study shows that γ-parvin is highly expressed in myeloid and lymphoid cells and that neither hematopoiesis nor T-cell-dependent antibody response, nor lymphocyte or dendritic cell (DC) migration is abnormal in the absence of γ-parvin.

## MATERIALS AND METHODS

**Antibodies.** Rabbit anti-PINCH1 and PINCH2 polyclonal antibodies were described (18). Monoclonal anti-ILK antibody was from BD Transduction Laboratory, rabbit anti-α-actin and mouse antitalin antibodies were from Sigma Aldrich, rat anti-B220 (RA3-6B2), rat anti-Thy1.2, anti-rabbit or -mouse immunoglobulin G (IgG) (H+L)–horseradish peroxidase, anti-IgM (R6-60.2), rat anti-IgD (11-26c.2a), rat anti-CD19 (1D3), anti-CD4 (H129.19), anti-CD8 (53-6.2), rat anti-CD3 (17A2), anti-Gr-1 (RB6-8C5), anti-Mac-1 (M1-70), anti-Ter-119, hamster anti-CD11c (HL3), CD86 (GL1), and major histocompatibility complex (MHC) II (M5/114.15.2) were from BD Pharmingen (San Jose, CA). Alexa 488 phalloidin was from Molecular Probes (Leiden, The Netherlands).

Antibodies were conjugated with fluorescein isothiocyanate (FITC), phycoerythrin (PE), or biotin and used at a 1:200 dilution. FITC-conjugated goat anti-rat or -mouse IgGs and streptavidin Cy-5 were from Jackson Immunoresearch (West Grove, PA). Rabbit pan-laminin antibody was described in Sorokin et al. (28). Annexin V-FITC was a gift from Ernst Pöschl (University of Erlangen-Nürnberg, Erlangen-Nürnberg, Germany) and was used at a 1:1,000 dilution.
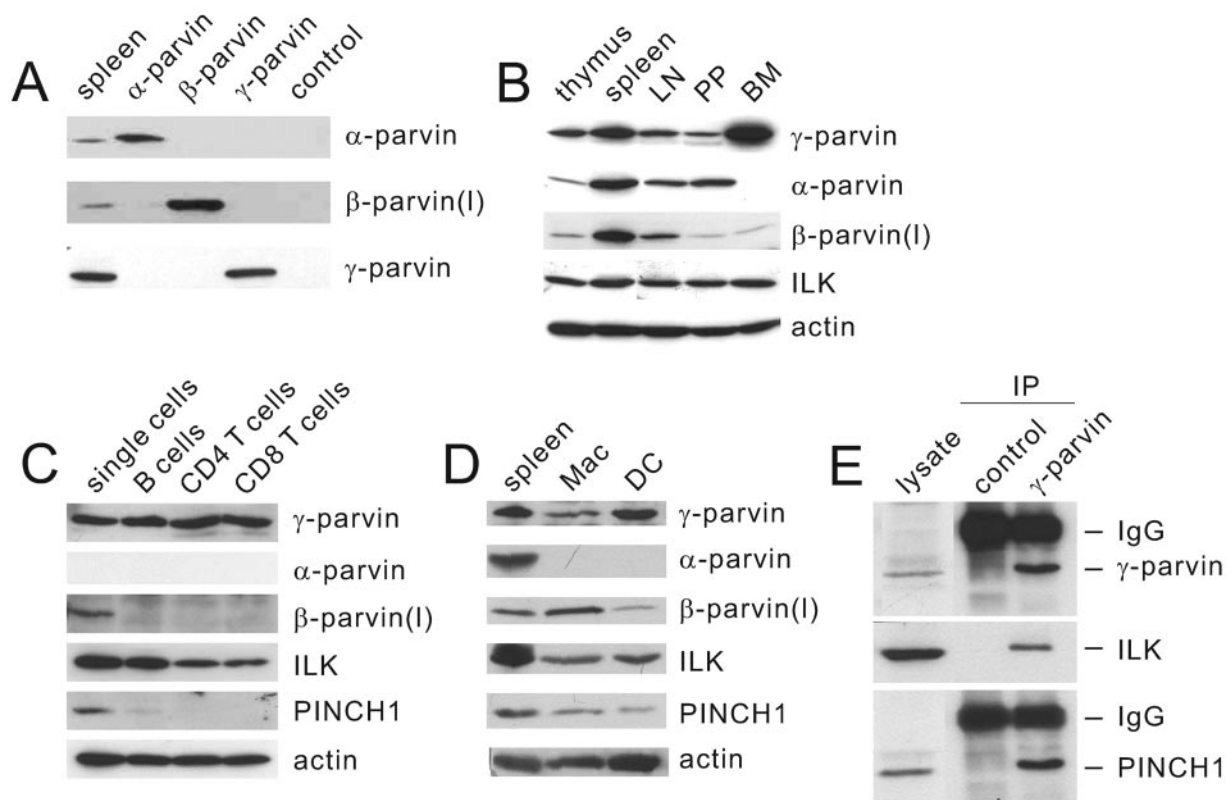
FIG. 1. Expression of parvins in the hematopoietic system (A) Peptide antisera were generated against α-parvin, the long isoform of β- and γ-parvin. Spleen lysate and in vitro-translated α-, β-, and γ-parvin proteins were subjected to sodium dodecyl sulfate-polyacrylamide gel electrophoresis and probed with the antisera. (B) Thymus, spleen, lymph nodes (LN), Peyer's (PP), and bone marrow (BM) were isolated, lysed, and immunoblotted with anti-γ-, α-, and β-parvin and anti-ILK antibodies. (C) B220-, CD4-, and CD8-positive cells were sorted from adult mouse splenic single cell suspensions and analyzed by Western blotting with antiparvin, anti-ILK, and anti-PINCH1 antibodies. (D) BM-derived macrophages (Mac) and dendritic cells (DCs) were lysed and immunoblotted with antiparvin, -ILK, and -PINCH1 antibodies. (E) BM-derived DC lysate was immunoprecipitated with anti-γ-parvin antibody and with control preimmune serum. The immunoprecipitates were immunoblotted with γ-parvin, ILK and PINCH1 antibodies, respectively.

**Generation of parvin peptide antibodies.** To generate specific antibodies, N-terminal peptides corresponding to α-parvin amino acid residues 5 to 19 (PQKSPLVPKSPTPKS), β-parvin residues 3 to 16 (SAPPRSPTPRAPKM), and γ-parvin residues 2 to 17 (ELEFLYDLLQLPKEVA) were synthesized, coupled to the carrier protein KLH (Imject Maleimide Activated mc KLH; Pierce), and used to immunize rabbits. The antisera were further purified by using the SulfoLink kit (Pierce) and tested on in vitro translated α-, β-, and γ-parvin proteins, respectively (Fig. 1A).

**Generation of γ-parvin-deficient mice.** A γ-parvin cDNA fragment derived from EST clone AA981356 was used to screen a 129/Sv mouse P1-derived artificial chromosome library (27). P1-derived artificial chromosome 656L16 (from the Human Genome Mapping Project Center, Cambridge, United Kingdom) was used to generate the targeting vector. A 5.5-kb fragment was used as 5′ flanking arm and a 2.3-kb fragment as a 3′ flanking arm (Fig. 2A). An internal ribosome entry site-*lacZ* reporter cassette, followed by a PKG-driven *neo* gene (27), was inserted between the two arms. The targeting vector was electroporated into passage 15 R1 embryonic stem (ES) cells and selected with G418 (3). Southern blots from 360 EcoRV-digested ES cell clones were hybridized with an external 700-bp SphI-HindIII fragment derived from intron 10 (Fig. 2A). Nine recombinant ES clones were identified by detection of a 4.9-kb recombinant band, in addition to the 5.7-kb wild-type band. Three targeted ES clones were injected into blastocysts to generate germ line chimeras, which were then mated with C57BL/6 females. Genotyping of γ-parvin mutant mice was performed by Southern blot or by PCR using a wild-type allele primer pair (forward, GTTTGAAGAACTGCA GAAGG; reverse, GTTGATCCATTCCATCAGCA) and a recombinant allele-specific primer pair derived from the *lacZ* gene (forward, CTGGGTAATAAG CGTTGGCAAT; reverse, CCAACTGGTAATGGTAGCGAC).

**In vitro translation.** α-, β-, and γ-parvin cDNAs (16) were amplified with Vent DNA polymerase (New England Biolabs, United Kingdom) and cloned into a modified pCS2⁺ mammalian SP6 promoter driven expression vector. In vitro translation reactions were performed with TNT Coupled Transcription/Translation Systems (Promega, Mannheim, Germany) using rabbit reticulocyte lysate and subsequently analyzed by Western assay.

**Western analysis and immunoprecipitation.** Cells were lysed in 150 mM NaCl–5 mM EDTA–1% Triton X-100 (pH 7.4) in the presence of protease inhibitors (Roche, Mannheim, Germany). Alternatively, tissues were homogenized in radioimmunoprecipitation assay buffer (150 mM NaCl, 50 mM Tris-HCl [pH 7.4], 5 mM EDTA, 0.1% sodium dodecyl sulfate, 1% sodium deoxycholate, 1% Triton X-100) containing protease inhibitors. For Western analysis, 30 to 50 µg of protein were gel separated, blotted, and probed with the primary and the secondary horseradish peroxidase-conjugated antibodies.

For immunoprecipitation, cells were lysed in ice-cold buffer (150 mM NaCl, 1 mM EGTA, 1% Triton X-100, 100 mM NaF, 10% glycerol, 50 mM HEPES [pH 7.5], 10 mM Na₄P₂O₇) supplemented with protease inhibitors. Then, 500 µg of protein was incubated with 0.8 mg of protein A (Sigma) in 50 µl of lysis buffer and with 1 µg of purified γ-parvin antibody or 1 µg of preimmune serum as a negative control at 4°C overnight. The protein-antibody-containing pellet was washed with lysis buffer and subjected to immunoblotting.

**Northern blot assay, reverse transcription-PCR (RT-PCR), and immuno-staining.** Preparation, gel separation, blotting, and hybridization of total RNA from spleen and thymus was performed as previously described (3). γ-Parvin cDNA (nucleotides 269 to 865) was used as probes.

For RT-PCR, total RNA was reverse-transcribed with iScript cDNA Synthesis Kit (Bio-Rad, Germany) and amplified with a β-parvin forward primer located in exon 5 (GGAAGCCGTGCAAGACCTGC) and a reverse primer located in exon 6 (CCCTGAAGTGCATGGCCAGG). An HPRT1 primer pair was used as a control (forward, TCAGTCAACGGGGGACATAAA; reverse, GGGGCT GTACTGCTTAACCAG).
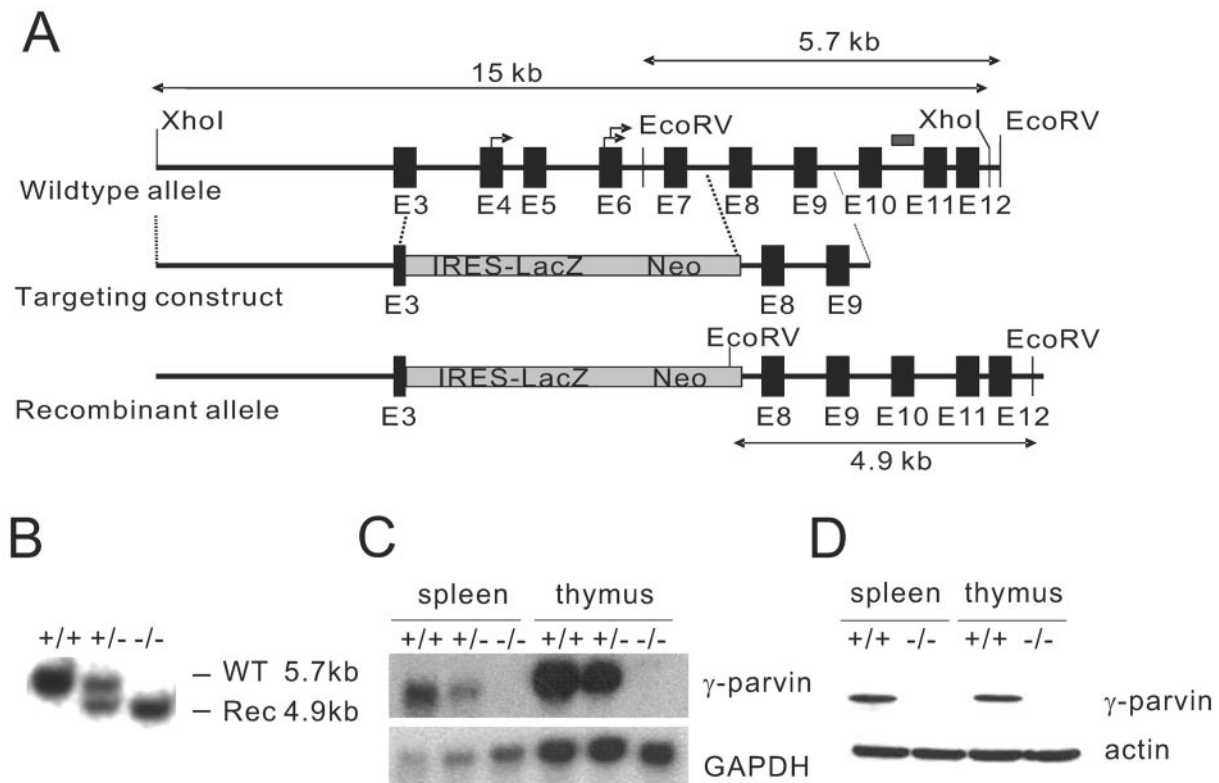
FIG. 2. Generation of γ-parvin-deficient mice. (A) An internal ribosome entry site (IRES)-LacZ neomycin cassette was inserted into the γ-parvin gene by replacing a 5.4-kb genomic fragment spanning exon 3 to intron 7, including both ATG-containing exons. The arrow indicates ATG triplets. (B) Homozygous mice were genotyped by Southern blot. (C) Loss of γ-parvin mRNA was shown by Northern blot in mouse thymus and spleen tissues. GAPDH cDNA probe was used to control mRNA loading. (D) Loss of γ-parvin expression was determined by Western blotting. The blots were reprobed with antiactin as loading control. Single cells, spleen single-cell suspension; WT, wild type; Rec, recombinant.

Immunofluorescence studies of tissue sections and cells were performed as described previously (3).

**Flow cytometry analysis (FACS) and magnetic cell sorting.** Single-cell suspensions were prepared by gently pushing the dissected organs through 70-mm cell strainers (BD). Fluorescence-activated cell sorting (FACS) analysis was performed as described previously (24). For magnetic cell sorting, $10^7$ spleen cells were mixed with FITC-conjugated anti-B220, CD4, CD8, or CD3 antibodies (BD Biosciences), respectively; incubated with anti-FITC microbeads; and sorted out according to the instructions of the manufacturer (Miltenyi Biotech, Inc.). Sorted cells were analyzed by FACS to test purities and analyzed by Western blotting or RT-PCR.

Generation of bone marrow (BM)-derived DC and macrophages were carried out as described previously (20, 26). Cells were immunostained (DCs for CD11c and Gr-1, macrophages for Mac-1) and analyzed by FACS.

For apoptosis assay, macrophages were harvested on day 8, stained with annexin V-FITC, and analyzed by FACS to determine the percentage of the apoptotic cells.

**DC migration in vivo.** On days 8 to 10 of DC culture, the medium was supplemented with 200 ng of lipopolysaccharide (LPS; Sigma)/ml to induce maturation. For fluorescence labeling, cells in phosphate-buffered saline were incubated for 10 min with 3 mM CFSE or 10 μM TAMRA (Molecular Probes) at room temperature. A 1:1 mixture of each $10^6$ CFSE- and TAMRA-labeled DC was injected into the hind footpad of recipient mice in a volume of 30 ml of phosphate-buffered saline. After 48 h, the popliteal lymph nodes (LN) were dissected and immunostained with pan-laminin antibody, or single-cell suspensions were prepared and analyzed by flow cytometry.

**Lymphocyte homing in vivo.** Spleen single-cell suspensions of knockout and control animals were prepared and erythrocytes were lysed. For fluorescence labeling, cells were incubated for 10 min with 1 mM CFSE or 20 μM TAMRA (Molecular Probes) at room temperature. A 1:1 mixture of each $2 \times 10^7$ CFSE- and TAMRA-labeled cells was injected intravenously. After 90 min and 24 h, lymphocytes were isolated from spleen and peripheral LN (inguinal, axial), and

the ratio of control to mutant cells in these organs was determined by FACS using simultaneous staining with antibodies to B220 or CD3.

**Immunization.** Mice were immunized via the intraperitoneal route with 100 μg of alum-precipitated NP$_{23}$-CG) and boosted with 10 mg/mouse 6 weeks after the first immunization. A total of 50 μl of blood was collected from each mouse at the indicated time points. Enzyme-linked immunosorbent assays (ELISAs) were carried out as described previously (10).

**Statistics.** The statistical analyzes of FACS and ELISA data were performed by using the Student *t* test. The *P* value for significance was set at 0.05.

## RESULTS

**Expression of the parvin family members in the hematopoietic system.** To determine the expression of the individual parvin family members, we generated peptide antisera that exclusively recognized the corresponding in vitro translated protein (Fig. 1A). The β-parvin mRNA can generate three isoforms depending on which translation initiation codon is used for protein translation (34). The peptide we used to generate our anti-β-parvin antibody is not present in the two shorter isoforms called β-parvin(s) and β-parvin(ss). Hence, the anti-β-parvin antibody exclusively recognizes the long β-parvin(l) isoform.

Western blot analysis of lysates derived from thymus, spleen, LN and Peyer's patch (PP) revealed that α-parvin, β-parvin, and γ-parvin are expressed at the expected molecular masses (around 42 kDa for α- and β-parvin and 37 kDa for γ-parvin) (Fig. 1B). BM lysates showed high expression levels of γ-par-

vin, low levels of β-parvin and no detectable α-parvin (Fig. 1B). In addition to the BM, we detected the γ-parvin protein in thymus, spleen, LN, and PP on Western blot (Fig. 1B). In addition to these hematopoietic organs, we found very weak γ-parvin signal in lung and hardly detectable signal in testis lysates (data not shown). To further determine the cell-type-specific expression of the parvin family members, we sorted B cells and CD4- and CD8-positive T cells from adult mouse spleen by using magnetic microbeads. The purities of the sorted cells ranged between 92 and 99% as analyzed with cell-type-specific antibodies by FACS (data not shown). γ-Parvin was expressed at similar levels in all three cell populations (Fig. 1C). α- and β-parvin(l) were absent from B and T cells (Fig. 1C). Lysates from a splenic single-cell suspension showed γ- and β-parvin(l) expression but no detectable α-parvin. BM-derived macrophages and DCs expressed γ- and β-parvin but no detectable α-parvin protein (Fig. 1D).

α- and β-parvin can bind ILK and together with PINCH1 form an ILK-PINCH-parvin complex (39, 40). To test whether γ-parvin has similar properties, lysates from DCs were immunoprecipitated with anti-γ-parvin antibody or preimmune serum. Subsequent Western blotting detected ILK, PINCH1, and γ-parvin in the anti-γ-parvin immunoprecipitates but not in the preimmune serum control (Fig. 1E), indicating that γ-parvin can also bind ILK and form a ternary complex with ILK and PINCH1.

**Mice lacking γ-parvin expression are viable and fertile.** To directly analyze γ-parvin in vivo, we introduced a constitutive null mutation into the γ-parvin gene of mice (Fig. 2A). Southern blot or PCR based genotyping of tail biopsies from 159 3-month-old mice revealed the presence of homozygous mice at the expected Mendelian ratio (Fig. 2B and data not shown). Northern and Western blot analysis confirmed the absence of γ-parvin in homozygous mutant mice (Fig. 2C and D). Both heterozygous and homozygous γ-parvin mutant mice were indistinguishable from their wild-type littermate controls. They were fertile and had a normal life span.

**Normal hematopoiesis in γ-parvin-deficient mice.** α- and β-parvin have been shown to modulate cell migration and cell survival (6, 31, 34, 40). To test whether γ-parvin has a similar function in vivo, we first determined the cellularity and the population sizes of different cell lineages in BM, thymus, spleen, LN, and PP of 5-month-old control and γ-parvin-null mice. The average cell numbers were similar between control and γ-parvin-deficient BM, thymus, and spleen. They were $(29.8 \pm 8.1) \times 10^6$ in control BM and $(35.1 \pm 11.1) \times 10^6$ in γ-parvin-null BM, $(37.1 \pm 10.6) \times 10^6$ in control thymus and $(40.2 \pm 12.1) \times 10^6$ in γ-parvin-null thymus and $(104.0 \pm 33.5) \times 10^6$ in control spleen and $(107.6 \pm 30.8) \times 10^6$ in γ-parvin-null spleen.

To determine the population sizes of different cell lineages we prepared single cell suspensions from lymphoid organs, immunostained them with different lineage markers (B-cell markers B220, IgM, IgD, and CD19; T-cell markers CD4, CD8, and CD3; erythrocyte marker Ter119; granulocyte marker Gr-1; macrophage marker Mac-1; natural killer cell markers Dx5 and NK1.1) and analyzed them by FACS. The relative numbers of the different cell types were similar in BM, thymus, spleen, LN, and PP between control and γ-parvin-null mice of 4, 8, and 20 weeks of age (Fig. 3A to C and data not shown).

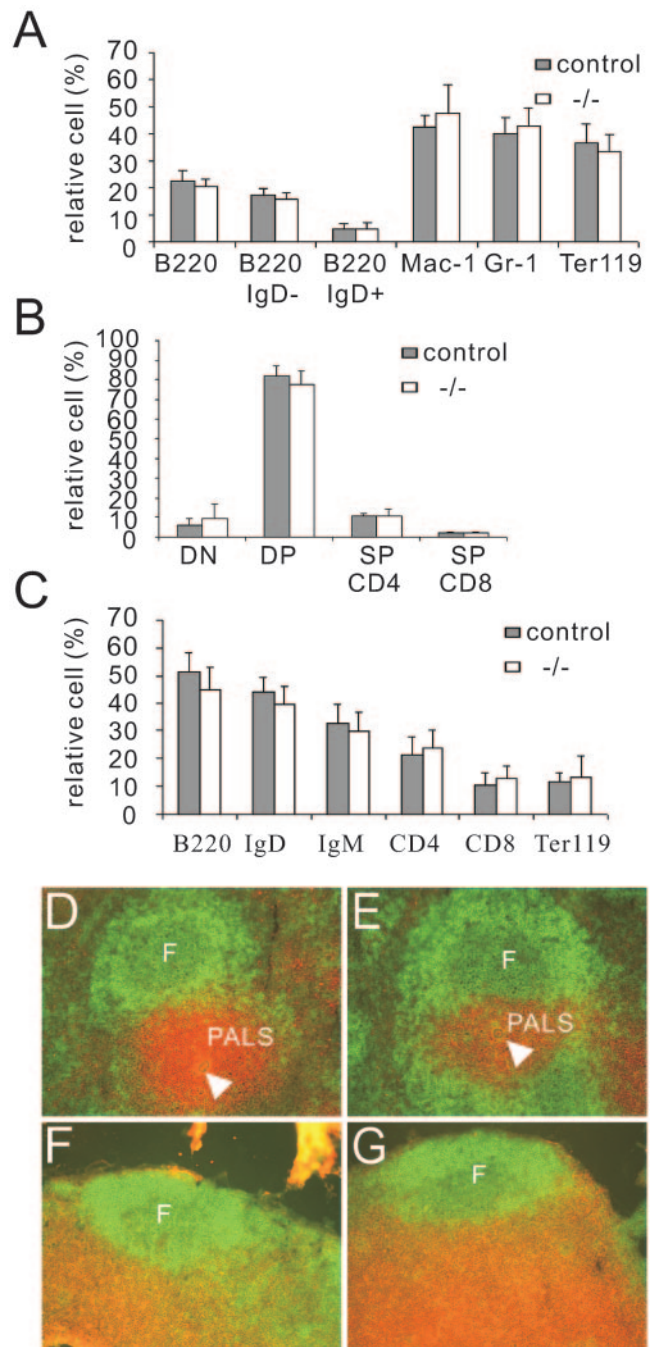

FIG. 3. Composition and architecture of lymphoid organs in γ-parvin-deficient mice. (A to C) Single-cell suspensions derived from primary and secondary lymphoid tissues (BM [A], thymus [B], spleen [C]) were immunostained with different hematopoietic lineage makers and analyzed by FACS. The relative cell numbers are shown (n = 5/5, 5-month-old mice). (D to G) Immunostaining of spleen (D and E) and LN (F and G) with anti-B220 (FITC) and anti-Thy1.2 (Cy3) antibodies showed normal distribution of B and T cells. F, B-cell follicle; PALS, periarteriolar lymphoid sheath. Magnification, ×200.

To test whether γ-parvin-null hematopoietic organs have a normal architecture and distribution of the different cell populations, we performed histochemistry and immunostainings of tissue sections derived from hematopoietic organs. Hematox-
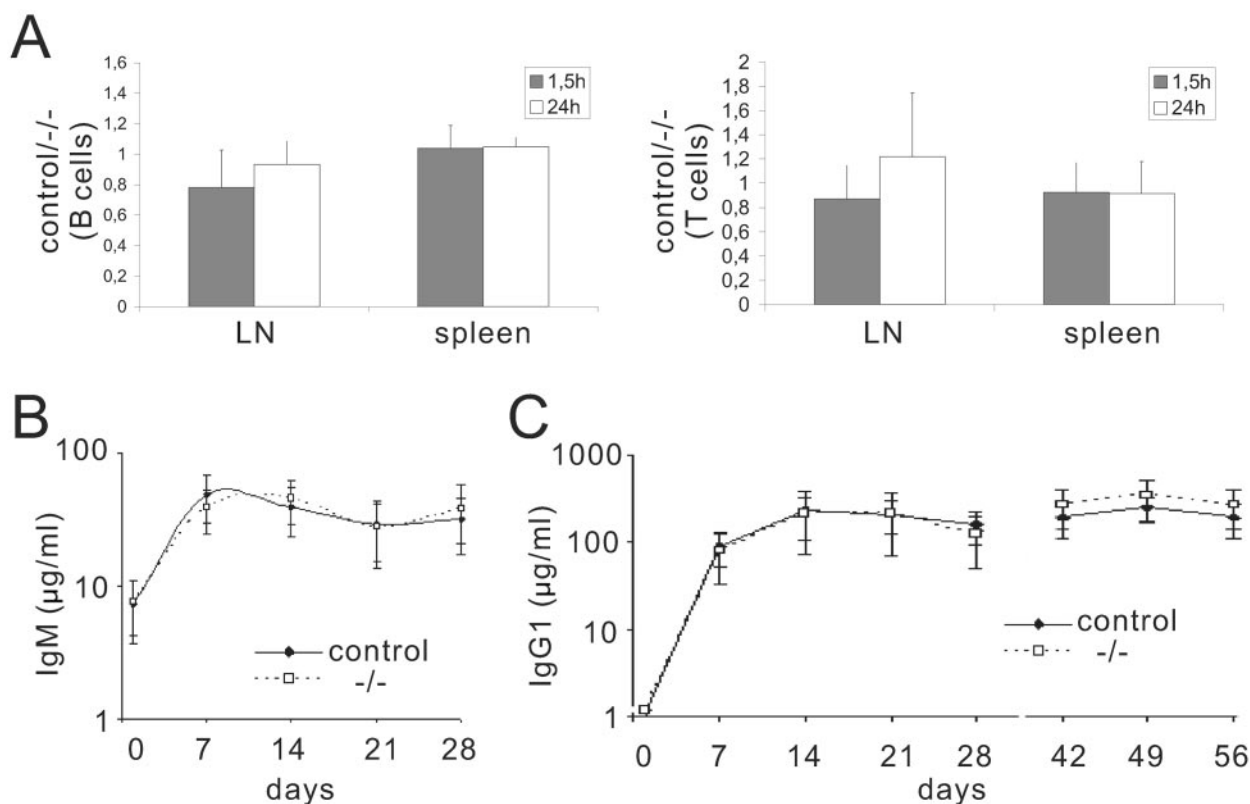
FIG. 4. Lymphocyte homing and T-cell-dependent antibody responses in γ-parvin-deficient mice. (A and B) Spleen single cell suspensions of γ-parvin-deficient and control mice were labeled with TAMRA and CFSE, mixed 1:1, and injected intravenously into wild-type mice. Half of the experiments were performed with inverted labeling. The ratio of knockout to control B and T cells in LN and spleen was determined by FACS. Values are the means of three independent experiments with three to six animals ± the standard error of the mean. (B and C) Mice were immunized with the T-cell-dependent antigen NP-CG, and the anti-NP IgM (B) and IgG1 (C) responses were measured by ELISA. ($n = 7$).

ylin-eosin staining revealed a normal architecture of thymus, spleen, LN, and PP derived from γ-parvin-null mice (data not shown). Immunostaining of spleen, LN, and PP with the B-cell marker B220 and the T-cell marker Thy1.2 showed normal T- and B-cell distribution in the mutant tissues (Fig. 3D and data not shown).

**Normal lymphocyte homing and T-cell-dependent antibody response in γ-parvin-deficient mice.** The association of γ-parvin with integrins and the actin cytoskeleton in hematopoietic cells suggested a potential role of γ-parvin in leukocyte trafficking. We therefore tested whether short and long-term homing of B and T cells was altered in the absence of γ-parvin. Single cell suspensions of spleens from knockout and control mice were labeled with different fluorescent dyes and a 1:1 mixture of both genotypes was injected intravenously into wild-type recipients. After 90 min and 24 h the ratio of fluorescent cells that homed into spleen and peripheral lymph nodes was determined for B220 positive B cells and CD3 positive T cells, respectively. No significant difference in homing frequency could be observed between mutant and control cells (Fig. 4A).

To more generally test for a role of γ-parvin in adaptive immune responses, we first measured the levels of total immunoglobulins (IgM, IgA, IgG1, IgG2a, IgG2b, and IgG3) and found that they were similar between γ-parvin-null and control animals (data not shown). Next, we investigated whether the T-cell-dependent antibody response differs between control

and γ-parvin-null mice. Mice were immunized with the T-cell-specific antigen NP-CG and the anti-NP antibody heavy chain isotypes (IgM and IgG1), as well as light-chain isotypes (Igκ and Igλ) were measured 1, 2, 3, and 4 weeks later by ELISA. No significant differences were found in any of these anti-NP isotypes between γ-parvin-null and control mice (Fig. 4B and C; see Fig. S1 in the supplemental material). Moreover, when mice were boosted with NP-CG antigens 6 weeks after the immunization, γ-parvin-null mice showed a similar memory antibody response as control mice (Fig. 4C and Fig. S1 in the supplemental material; data for IgG2a and IgG3 are not shown).

**Differentiation of macrophages and maturation and migration of DCs are normal in γ-parvin-deficient mice.** To test for a possible role of γ-parvin in the myeloid lineage, we differentiated DCs from BM precursors in vitro and induced maturation by adding LPS to the culture medium. Efficiency of DC generation was identical in γ-parvin-deficient and control cultures (Fig. 5A). Morphology as determined by bright-field microscopy was unchanged in this cell type (data not shown). To more specifically address possible cytoskeletal alterations, we performed immunostaining of adherent immature DC for F-actin and the integrin-associated proteins talin (Fig. 5B) and vinculin (not shown). Independent of the genotype, we found the typical podosome structure containing an actin core surrounded by a ring of talin and vinculin.
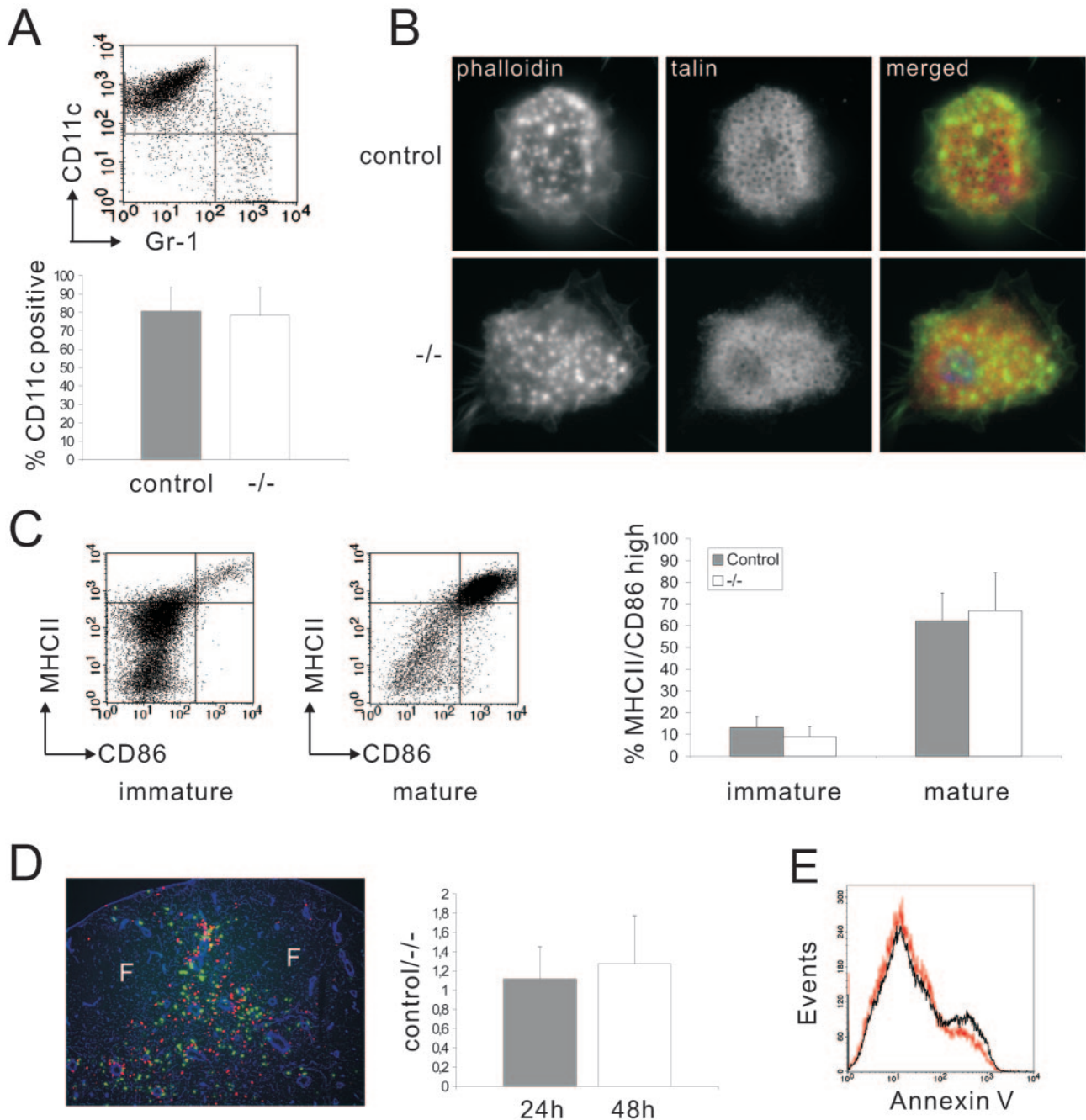
FIG. 5. Differentiation, maturation, and migration of BM-derived DCs. (A) γ-Parvin control and null BM-derived DCs were analyzed by FACS with CD11c and Gr-1 antibodies. Quantification shows mean values of three independent experiments. (B) Immature DC were plated on coverslips, fixed, and immunostained. (C) FACS analysis of MHCII and CD86 on the BM-derived DCs (upper panel) and mature DCs stimulated with LPS overnight (lower panel). The quantification shows mean values of three independent experiments ± the SD. (D) BM-derived DCs from both control and γ-parvin-deficient mice were stimulated with LPS overnight, labeled with TAMRA and CFSE, respectively, mixed in a 1:1 ratio, and subsequently injected into the hind footpad of mice. After 48 h, the popliteal LNs were dissected and immunostained with pan-laminin antibody. F, B-cell follicle. Magnification, ×200. Quantitative data were obtained by FACS analysis of popliteal lymph nodes. Values are means of five independent experiments with three to six mice each ± the standard error of the mean. (E) BM-derived macrophages were harvested (including the cells in suspension) on day 8 and stained with FITC-conjugated annexin V. Data for control cells are shown in black line; those for γ-parvin-null cells are shown in red.

After maturation, γ-parvin-deficient DCs upregulated MHC II and the costimulatory molecules CD86 and CD40 to a similar extent as control DCs (Fig. 5C and data not shown). In vivo, these mature DCs actively migrate via the afferent lymphatics into the draining LNs where they encounter and activate naive T cells. To test migration and positioning of DC in vivo, we performed competitive migration experiments. In vitro generated γ-parvin-deficient, and control DCs were la-
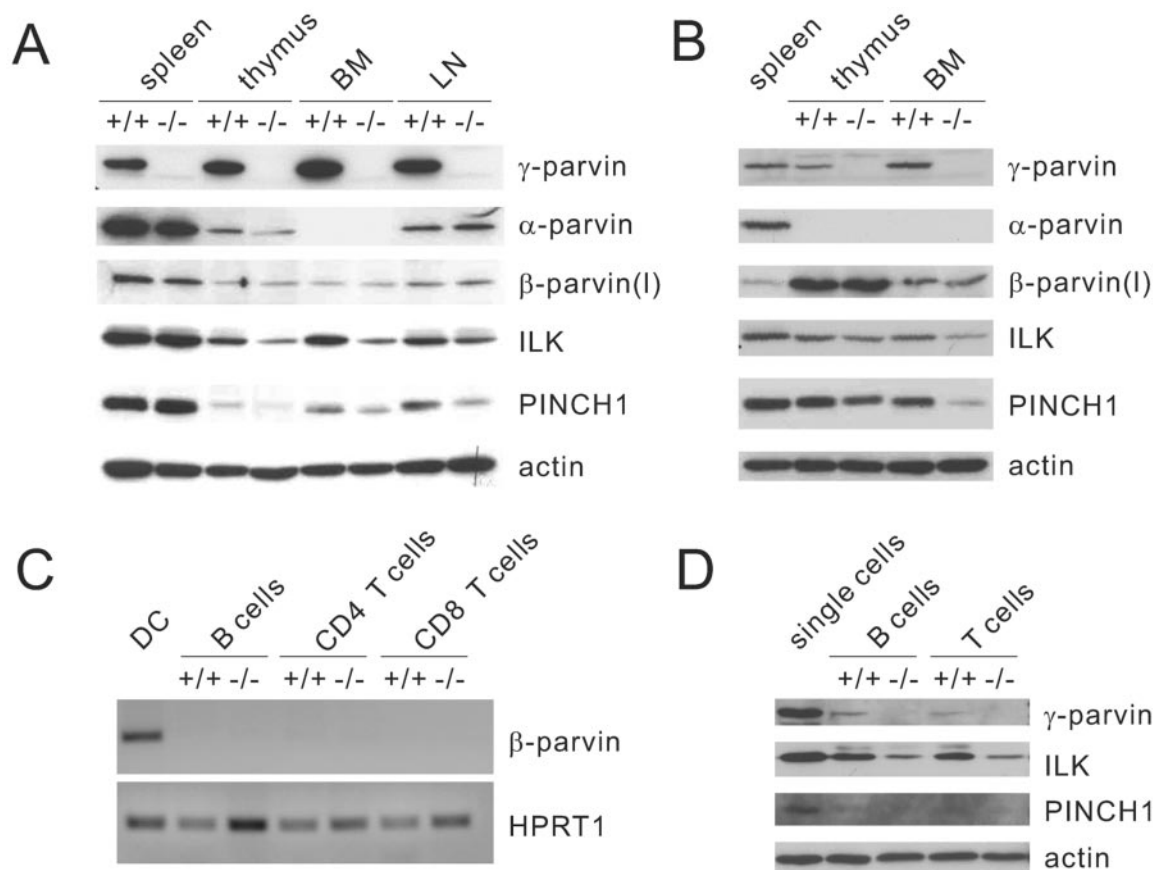
FIG. 6. Levels of α- or β-parvin in γ-parvin-deficient mice. (A) The lysates derived from spleen, thymus, BM, and LN from both control and γ-parvin-deficient mice were immunoblotted with anti-parvin, ILK, and PINCH1 antibodies. (B) BM-derived macrophages and DCs from both control and γ-parvin-deficient mice were immunoblotted with antiparvin, anti-ILK, and anti-PINCH1 antibodies. (C) B220-, CD4-, and CD8-positive cells were sorted from adult splenic single cells and analyzed by RT-PCR for β-parvin mRNA. HPRT1 was used as a control. (D) B220- and CD3-positive cells were sorted from adult splenic single cells and analyzed by Western blotting with anti-γ-parvin, -ILK, and -PINCH1 antibodies. BM, bone marrow; LN, lymph nodes; Mac, macrophages; DC, dendritic cells.

beled with different fluorescent dyes, mixed at a 1:1 ratio, and injected into the footpads of wild-type mice. Histological examination of the draining LNs 24 and 48 h after injection revealed that both γ-parvin-null and control DCs migrated into the T-cell cortex where they located in the same areas (Fig. 5D and data not shown). For quantification, LN suspensions were analyzed by flow cytometry revealing no significant differences between knockout and control cells. These data indicate that myelopoiesis, terminal maturation, and migration of DCs are unaltered in the absence of γ-parvin.

It has been shown that deletion of ILK in a macrophage cell line resulted in increased apoptosis due to decreased levels of PKB/Akt phosphorylation (29). To test whether this effect could be due to the absence of the ILK-PINCH-γ-parvin complex, we differentiated primary macrophages from BM precursor cells in vitro and stained for annexin V to determine the percentage of apoptotic cells in the cultures. Our data showed that γ-parvin-null BM precursors could differentiate into macrophages, as well as heterozygous control cells, and both purities were more than 98% (FACS data not shown). No difference in apoptosis could be

observed between γ-parvin-null and heterozygous control cells (data not shown and Fig. 5E).

**Loss of γ-parvin is not compensated by an upregulation of α- or β-parvin expression.** It is possible that the lack of an obvious phenotype in the hematopoietic organs and in T and B cells, and DCs of mutant mice is due to compensation by other parvin family members. To test this hypothesis, we determined the expression of all parvins in hematopoietic organs and myeloid and lymphoid lineages. The level of the β-parvin(l) isoform (that is detected by our antibody) was unchanged in the γ-parvin-deficient BM, thymus, spleen, and LN (Fig. 6A), as well as in macrophages and DCs (Fig. 6B). To exclude expression of the shorter isoforms in T and B cells, we performed RT-PCR and found that β-parvin mRNA was not detectable in both control and γ-parvin-deficient cells (Fig. 6C), indicating that also the smaller isoforms are not compensating for the loss of γ-parvin. The level of α-parvin protein was neither increased in lysates from mutant thymus nor mutant LN nor spleen (Fig. 6A), and undetectable in γ-parvin-deficient, as well as wild-type BM, DCs, and macrophages (Fig. 6B).

Next we tested whether the absence of γ-parvin had an impact on the ternary protein complex with ILK and PINCH1. Western blot analyzes showed that ILK and PINCH1 proteins were reduced in the γ-parvin-deficient BM, thymus, spleen, and LN (Fig. 6A), as well as in γ-parvin-deficient macrophages and DCs (Fig. 6B). In B and T lymphocytes, ILK protein was also reduced, while PINCH1 was undetectable in B and T cells in the absence of γ-parvin (Fig. 6D).

## DISCUSSION

In the present study we report the hematopoietic expression pattern of the parvin family members, show that γ-parvin can form a ternary complex with ILK and PINCH1, and describe the first analysis of γ-parvin-deficient mice.

To determine the expression of the individual parvin members in hematopoietic organs and cells, we used peptides to generate highly specific antibodies against α-, β-, and γ-parvin. Western analysis with these antibodies showed that γ-parvin was the only parvin family member that was expressed in all hematopoietic organs and cells tested. γ-Parvin is highly expressed in B and T lymphocytes, DCs, and, to a lesser extent, in macrophages. β-Parvin was expressed in all hematopoietic organs, in myeloid cells but not in lymphocytes. Finally, our Western blot studies showed that α-parvin was present in whole organ lysates derived from spleen, thymus and LN but absent in splenic single cells, BM-derived cells, and myeloid (DCs and macrophages) and lymphoid cells (T and B lymphocytes). These findings suggest that α-parvin is likely expressed in stromal and/or endothelial cells of hematopoietic organs and may have, if at all, a rather indirect role on the development and function of hematopoietic cells.

It has been shown in several studies that α- and β-parvins localize to focal adhesion sites and tensin-rich fibrillar adhesions (11, 23, 31, 34). A central player for recruiting α- and β-parvin to focal adhesions is ILK, which binds with its kinase domain to the second calponin homology domain of the α- or β-parvins and with its N-terminal ankyrin repeat to the LIM only protein PINCH (30, 31, 34). The ternary protein complex of ILK, PINCH, and α- or β-parvin forms prior to cell adhesion and is anchored through ILK to the cytoplasmic domain of the β1 integrin upon adhesion (33, 34, 39, 40). γ-Parvin shares approximately 40% identity and 60% similarity with the paralogous α- and β-parvins, and it was not known whether γ-parvin is also capable of binding ILK and forming a complex with PINCH. To resolve this question, we performed coimmunoprecipitation experiments with lysates from DCs, which express high levels of ILK, PINCH1, and γ-parvin. The results revealed that immunoprecipitation of γ-parvin efficiently pulled down ILK and PINCH1, indicating that γ-parvin can, like the other parvins, form and stabilize a ternary complex with ILK and PINCH1.

The specific expression of γ-parvin in hematopoietic cells suggests a potential role in hematopoiesis and/or the immune response. Furthermore, the ability to associate with ILK and PINCH1 makes γ-parvin and the entire ternary protein complex a candidate for transducing β1 and β3 integrin functions in hematopoietic cells. β1 integrins are expressed on almost all hematopoietic cells and perform functions during the embryonic and adult hematopoiesis. During embryogenesis β1 integrins control trafficking of embryonic and extra-embryonic hematopoietic stem cells into the fetal liver (13, 24) and induce the formation of PPs by enabling the interaction of a unique subset of hematopoietic cells that is expressing CD4 and lacking CD3 with stromal cells in the gut (4). Postnatally, β1 integrins are essential for the homing of adult hematopoietic stem cells into the BM and the regulation of the T-cell-dependent antibody response (1, 2, 24). β3 integrins have an essential role for platelet aggregation (14) and play a more subtle role during monocyte migration (32). The role of ILK and PINCH1 in blood cells is less well studied. In one report it has been demonstrated that ILK plays an important role for monocyte/macrophage survival by regulating the activation of PKB/Akt (29), and another study suggested that ILK may regulate transendothelial migration of monocytes (5). To test whether γ-parvin contributes, at least in part, to the transduction of the β1 and/or β3 integrin function(s) in the hematopoietic system, we disrupted the γ-parvin gene in mice. Surprisingly, the γ-parvin-deficient mice were born at the expected Mendelian distribution, were fertile, and displayed no obvious phenotype. Moreover, the cell numbers and the proportion of different myeloid and lymphoid cells in BM, thymus, spleen, LN, and PP were normal in mice lacking γ-parvin expression. Similarly, differentiation of BM precursors to macrophages occurred normally and without signs of increased apoptosis. This indicates that γ-parvin has no rate-limiting function for the homing of hematopoietic stem cells during development, as well as for their potential to give rise to the different blood cell lineages. Furthermore, the recirculation through lymphatic organs is also normal in the absence of γ-parvin. Finally, functional assays such as T-cell-dependent antibody response and the in vivo migration of BM-derived DCs to LN are also independent of the expression of γ-parvin.

An explanation for the lack of phenotype in γ-parvin-deficient mice is compensation or redundancy by other parvin family members. Although this could explain the normal migration of DCs and the absence of apoptosis in macrophages, which both express in addition to γ-parvin significant levels of β-parvin, it does not explain the normal T-cell-dependent antibody response, since both T and B cells express γ-parvin only and neither upregulate α- nor β-parvin expression in the absence of γ-parvin. In line with previous studies on the stability of the ILK/PINCH/parvin complex, the loss of γ-parvin expression reduced the levels of ILK and PINCH in T cells (33). Interestingly, the reduction of ILK and PINCH1 in γ-parvin-deficient T and B cells suggests that the ILK/PINCH1/γ-parvin complex plays most likely a more subtle role for regulating the T-cell-dependent antibody response and that β1 integrins use another signaling complex to fulfill this task. Such functions can be tested by deleting individual members of the ILK/PINCH/parvin complex specifically in T cells using the Cre/loxP system.

In summary, our study shows that mouse development and postnatal aging can proceed normally when the γ-parvin gene is disrupted. Although the γ-parvin gene seems to be dispensable in vivo, we cannot rule out that γ-parvin serves specific tasks that we have not been investigated here. It is also possible that there is a certain degree of compensation between γ-parvin and β-parvin. This possibility will be difficult to analyze, since the γ-parvin and β-parvin genes are separated by only

around 12 kb and the generation of compound mutant mice is only possible by targeting both genes in the same ES cell line.

## ACKNOWLEDGMENTS

## REFERENCES

1. **Brakebusch, C., and R. Fässler.** 2003. The integrin-actin connection, an eternal love affair. EMBO J. **22:**2324–2333.
2. **Brakebusch, C., S. Fillatreau, A. J. Potocnik, G. Bungartz, P. Wilhelm, M. Svensson, P. Kearney, H. Korner, D. Gray, and R. Fässler.** 2002. β1 integrin is not essential for hematopoiesis but is necessary for the T cell-dependent IgM antibody response. Immunity **16:**465–477.
3. **Fässler, R., M. Pfaff, J. Murphy, A. A. Noegel, S. Johansson, R. Timpl, and R. Albrecht.** 1995. Lack of β1 integrin gene in embryonic stem cells affects morphology, adhesion, and migration but not integration into the inner cell mass of blastocysts. J. Cell Biol. **128:**979–988.
4. **Finke, D., H. Acha-Orbea, A. Mattis, M. Lipp, and J. Kraehenbuhl.** 2002. CD4+ CD3- cells induce Peyer's patch development: role of alpha4beta1 integrin activation by CXCR5. Immunity **17:**363–373.
5. **Friedrich, E. B., S. Sinha, L. Li, S. Dedhar, T. Force, A. Rosenzweig, and R. E. Gerszten.** 2002. Role of integrin-linked kinase in leukocyte recruitment. J. Biol. Chem. **277:**16371–16375.
6. **Fukuda, T., L. Guo, X. Shi, and C. Wu.** 2003. CH-ILKBP regulates cell survival by facilitating the membrane translocation of protein kinase B/Akt. J. Cell Biol. **160:**1001–1008.
7. **Fukuda, T., K. Chen, X. Shi, and C. Wu.** 2003. PINCH-1 is an obligate partner of integrin-linked kinase (ILK) functioning in cell shape modulation, motility, and survival. J. Biol. Chem. **278:**51324–51333.
8. **Geiger, B., A. Bershadsky, R. Pankov, and K. M. Yamada.** 2001. Transmembrane crosstalk between the extracellular matrix-cytoskeleton crosstalk. Nat. Rev. Mol. Cell. Biol. **2:**793–805.
9. **Grashoff, C., I. Thievessen, K. Lorenz, S. Ussar, and R. Fässler.** 2004. Integrin-linked kinase: integrin's mysterious partner. Curr. Opin. Cell Biol. **16:**565–571.
10. **Gray, D., P. Dullforce, and S. Jainandunsing.** 1994. Memory B-cell development but not germinal center formation is impaired by in vivo blockade of CD40-CD40 ligand interaction. J. Exp. Med. **180:**141–155.
11. **Guo, L., and C. Wu.** 2002. Regulation of fibronectin matrix deposition and cell proliferation by the PINCH-ILK-CH-ILKBP complex. FASEB J. **16:**1298–1300.
12. **Guo, W., and F. G. Giancotti.** 2004. Integrin signalling during tumour progression. Nat. Rev. Mol. Cell. Biol. **5:**816–826.
13. **Hirsch, E., A. Iglesias, A. J. Potocnik, U. Hartmann, and R. Fässler.** 1996. Impaired migration but not differentiation of hematopoietic stem cells in the absence of β1 integrins. Nature **380:**171–175.
14. **Hodiva-Dilke, K. M., K. P. McHugh, D. A. Tsakiris, H. Rayburn, D. Crowley, M. Ullman-Cullere, F. P. Ross, B. S. Coller, S. Teitelbaum, and R. O. Hynes.** 1999. β3-Integrin-deficient mice are a model for Glanzmann thrombasthenia showing placental defects and reduced survival. J. Clin. Investig. **103:**229–238.
15. **Hynes, R. O.** 2002. Integrins: bidirectional, allosteric signaling machines. Cell **110:**673–687.
16. **Korenbaum, E., T. M. Olski, and A. A. Noegel.** 2001. Genomic organization and expression profile of the parvin family of focal adhesion proteins in mice and humans. Gene **279:**69–79.
17. **Lee, J. W., and R. Juliano.** 2004. Mitogenic signal transduction by integrin- and growth factor receptor-mediated pathways. Mol. Cells **17:**188–202.
18. **Li, S., R. Bordoy, F. Stanchi, M. Moser, A. Braun, O. Kudlacek, U. M. Wewer, P. D. Yurchenco, and R. Fässler.** 2005. PINCH1 regulates cell-matrix and cell-cell adhesions, cell polarity and cell survival during the peri-implantation stage. J. Cell Sci. **118:**2913–2921.
19. **Lin, X., H. Qadota, D. G. Moerman, and B. D. Williams.** 2003. *Caenorhabditis elegans* PAT-6/actopaxin plays a critical role in the assembly of integrin adhesion complexes in vivo. Curr. Biol. **13:**922–932.
20. **Lutz, M. B., N. Kukutsch, A. L. Ogilvie, S. Rossner, F. Koch, N. Romani, and G. Schuler.** 1999. An advanced culture method for generating large quantities of highly pure dendritic cells from mouse bone marrow. J. Immun. Methods **223:**77–92.
21. **Mishima, W., A. Suzuki, S. Yamaji, R. Yoshimi, A. Ueda, T. Kaneko, J. Tanaka, Y. Miwa, S. Ohno, and Y. Ishigatsubo.** 2004. The first CH domain of affixin activates Cdc42 and Rac1 through αPIX, a Cdc42/Rac1-specific guanine nucleotide exchanging factor. Genes Cells **9:**193–204.
22. **Nikolopoulos, S. N., and C. E. Turner.** 2000. Actopaxin, a new focal adhesion protein that binds paxillin LD motifs and actin and regulates cell adhesion. J. Cell Biol. **151:**1435–1448.
23. **Olski, T. M., A. A. Noegel, and E. Korenbaum.** 2001. Parvin, a 42 kDa focal adhesion protein, related to the α-actinin superfamily. J. Cell Sci. **114:**525–538.
24. **Potocnik, A. J., C. Brakebusch, and R. Fässler.** 2000. Fetal and adult hematopoietic stem cells require β1 integrin function for colonizing fetal liver, spleen, and bone marrow. Immunity **12:**653–663.
25. **Rosenberger, G., I. Jantke, A. Gal, and K. Kutsche.** 2003. Interaction of alphaPIX (ARHGEF6) with beta-parvin (PARVB) suggests an involvement of alphaPIX in integrin-mediated signaling. Hum. Mol. Genet. **12:**155–167.
26. **Rutherford, M. S., and L. B. Schook.** 1992. Differential immunocompetence of macrophages derived using macrophage or granulocyte-macrophage colony-stimulating factor. J. Leukoc. Biol. **51:**69–76.
27. **Sakai, T., S. Li, D. Docheva, C. Grashoff, K. Sakai, K. Kostka, A. Braun, A. Pfeifer, P. D. Yurchenco, and R. Fässler.** 2003. Integrin-linked kinase (ILK) is required for polarizing the epiblast, cell adhesion, and controlling actin accumulation. Genes Dev. **17:**926–940.
28. **Sorokin, L., A. Sonnenberg, M. Aumailley, R. Timpl, and P. Ekblom.** 1990. Recognition of the laminin E8 cell-binding site by an integrin possessing the alpha 6 subunit is essential for epithelial polarization in developing kidney tubules. J. Cell Biol. **111:**1265–1273.
29. **Troussard, A. A., N. M. Mawji, C. Ong, A. Mui, R. St. Arnaud, and S. Dedhar.** 2003. Conditional knockout of integrin-linked kinase demonstrates an essential role in protein kinase B/Akt activation. J. Biol. Chem. **278:**22374–22378.
30. **Tu, Y., F. Li, S. Goicoechea, and C. Wu.** 1999. The LIM-only protein PINCH directly interacts with integrin-linked kinase and is recruited to integrin-rich sites in spreading cells. Mol. Cell. Biol. **19:**2425–2434.
31. **Tu, Y., Y. Huang, Y. Zhang, Y. Hua, and C. Wu.** 2001. A new focal adhesion protein that interacts with integrin-linked kinase and regulates cell adhesion and spreading. J. Cell Biol. **153:**585–598.
32. **Weerasinghe, D., K. P. McHugh, F. P. Ross, E. J. Brown, R. H. Gisler, and B. A. Imhof.** 1998. A role for the αvβ3 integrin in the transmigration of monocytes. J. Cell Biol. **142:**595–607.
33. **Wu, C.** 2004. The PINCH-ILK-parvin complexes: assembly, functions, and regulation. Biochim. Biophys. Acta **1692:**55–62.
34. **Yamaji, S., A. Suzuki, Y. Sugiyama, Y. Koide, M. Yoshida, H. Kanamori, H. Mohri, S. Ohno, and Y. Ishigatsubo.** 2001. A novel integrin-linked kinase-binding protein, affixin, is involved in the early stage of cell-substrate interaction. J. Cell Biol. **153:**1251–1264.
35. **Yamaji, S., A. Suzuki, H. Kanamori, W. Mishima, R. Yoshimi, H. Takasaki, M. Takabayashi, K. Fujimaki, S. Fujisawa, S. Ohno, and Y. Ishigatsubo.** 2004. Affixin interacts with α-actinin and mediates integrin signaling for reorganization of F-actin induced by initial cell-substrate interaction. J. Cell Biol. **165:**539–551.
36. **Yang, Y., L. Guo, S. M. Blattner, P. Mundel, M. Kretzler, and C. Wu.** 2005. Formation and phosphorylation of the PINCH-1-integrin linked kinase–α-parvin complex are important for regulation of renal glomerular podocyte adhesion, architecture, and survival. J. Am. Soc. Nephrol. **16:**1966–1976.
37. **Zhang, Y., K. Chen, L. Guo, and C. Wu.** 2002. Characterization of PINCH-2, a new focal adhesion protein that regulates the PINCH-1-ILK interaction, cell spreading, and migration. J. Biol. Chem. **277:**38328–38333.
38. **Zhang, Y., L. Guo, K. Chen, and C. Wu.** 2002. A critical role of the PINCH-integrin-linked kinase interaction in the regulation of cell shape change and migration. J. Biol. Chem. **277:**318–326.
39. **Zhang, Y., K. Chen, Y. Tu, A. Velyvis, Y. Yang, J. Qin, and C. Wu.** 2002. Assembly of the PINCH-ILK-CH-ILKBP complex precedes and is essential for localization of each component to cell-matrix adhesion sites. J. Cell Sci. **115:**4777–4786.
40. **Zhang, Y., K. Chen, Y. Tu, and C. Wu.** 2004. Distinct roles of two structurally closely related focal adhesion proteins, α-parvins and β-parvins, in regulation of cell morphology and survival. J. Biol. Chem. **279:**41695–41705.